Knockdown of circ_NEK6 Decreased ^{131}I Resistance of Differentiated Thyroid Carcinoma via Regulating miR-370-3p/MYH9 Axis

Fukun Chen[1], Shuting Yin[2], Zhiping Feng[1], Chao Liu[1], Juan Lv[1], Yuanjiao Chen[1], Ruoxia Shen[1], Jiaping Wang[3], and Zhiyong Deng[1] ⊙

Abstract

Radioresistance is a crucial factor for the failure of iodine 131 (^{131}I)-based radiotherapy for differentiated thyroid carcinoma (DTC). This study aimed to explore the effect of circ_NEK6 on the development of ^{131}I resistance in DTC and its potential mechanism. In this study, we demonstrated that circ_NEK6 expression was significantly elevated in ^{131}I-resistant DTC tissues and cell lines. Knockdown of circ_NEK6 significantly repressed ^{131}I resistance via inhibiting cell proliferation, migration, invasion abilities, and inducing cell apoptosis and DNA damage in ^{131}I-resistant DTC cells. Mechanistically, knockdown of circ_NEK6 suppressed ^{131}I resistance in DTC by upregulating the inhibitory effect of miR-370-3p on the expression of myosin heavy chain 9 (MYH9). *In vivo* experiments showed that circ_NEK6 inhibition aggravated ^{131}I radiation-induced inhibition of xenograft tumor growth. Taken together, knockdown of circ_NEK6 repressed ^{131}I resistance in DTC cells by regulating the miR-370-3p/MYH9 axis, indicating that circ_NEK6 may act as a potential biomarker and therapeutic target for DTC patients with ^{131}I resistance.

Keywords

Abbreviations

Introduction

Thyroid cancer is one of the most common malignant tumors of the endocrine system, with steadily increasing morbidity and mortality rates.[1] Differentiated thyroid cancer (DTC) is the main form of thyroid cancer, with the highest morbidity rate and accounts for approximately 80% of all thyroid cancer.[2] Surgery and radioiodine treatment after surgical intervention are the standard treatment methods for thyroid cancer,[3] but the postoperative recurrence rate of thyroid cancer is up to 23-30% according to epidemiologic investigations, indicating that the recurrence risk of the disease cannot be underestimated.[4,5] Iodine 131 (^{131}I)-based radiotherapy is commonly employed for clinical option, whereas ^{131}I resistance becomes a huge

[1] Department of Nuclear Medicine, Yunnan Cancer Hospital & The Third Affiliated Hospital of Kunming Medical University, Yunnan, China
[2] Department of Urology, The Second Affiliated Hospital of Kunming Medical University, Yunnan, China
[3] Department of Radiology, The Second Affiliated Hospital of Kunming Medical University, Yunnan, China

Corresponding Authors:
Zhiyong Deng, Department of Nuclear Medicine, Yunnan Tumor Hospital & The Third Affiliated Hospital of Kunming Medical University, No. 519 Kunzhou Road, Kunming 650118, Yunnan, China.
Email: zydeng22@163.com

Jiaping Wang, Department of Radiology, The Second Affiliated Hospital of Kunming Medical University, No. 1 Mayuan Road, Kunming 650000, Yunnan, China.
Email: jiapingwang12@163.com

challenge for treatment of patients with DTC,[6] as well as many of these patients will never be cured with radioactive iodine therapy and will become radioactive iodine refractory with a 3-year overall survival rate of less than 50%.[7] Hence, it is necessary to identify novel targets to improve ^{131}I sensitivity in DTC.

Circular RNA (circRNA) is a large class of endogenous non-coding RNAs (ncRNAs) with regulatory ability, extracellular stability, and evolutional conservation and plays a crucial role in gene regulation.[8] Numerous studies have shown the potential of circRNA to act as a biomarker for the diagnosis or prognosis of human diseases.[9] Additionally, previous studies have shown that many differentially expressed circRNAs can be screened using high-throughput sequencing[10] or microarrays.[11] Importantly, our previous study demonstrated that circ_NEK6 was upregulated in thyroid cancer tissues and cell lines, and circ_NEK6 inhibition significantly suppressed the malignant biological behavior of thyroid cancer cells.[12] However, to date, it remains unclear whether and how circ_NEK6 can regulate ^{131}I resistance in DTC.

microRNAs (miRNAs) are also potential regulators of tumor cells that are small ($\sim$22 nucleotides in length) non-coding, single-stranded RNAs that modulate the expression of various target genes. They regulate target genes by binding to the 3'-untranslated region (3'UTR) of the corresponding mRNA to form silencing complexes.[13] During the proliferation, migration, and invasion of tumor cells, it has been demonstrated that miRNAs act as oncogenes and tumor-suppressor genes. Further research has indicated that miRNAs exert opposing roles in different types of tumor cells.[14] For example, miR-370-3p exert diverse effects on the proliferation, apoptosis, invasion, and metastasis of various types of cancers.[15] In bladder cancer cell lines, miR-370-3p suppressed cell proliferation, migration, and invasion via targeting SOX12.[16] In thyroid cancer cells, miR-370-3p functions as a tumor-suppressor gene that inhibits cancer cell proliferation and metastasis, as well as induced cell apoptosis through the down-regulation of Frizzled class receptor 8 (FZD8).[12] Furthermore, myosin heavy chain 9 (MYH9) is an oncogene in human cancer,[17] and bioinformatics analysis has identified it as the target gene of miR-370-3p. Nevertheless, it is not known whether miR-370-3p can target MYH9 to regulate ^{131}I resistance and whether the miR-370-3p/MYH9 axis is required for the function of circ_NEK6 in the development of radioiodine resistance in DTC.

In this study, we examined the expression levels of circ_NEK6, miR-370-3p, and MYH9 in DTC tissues and cell lines. Moreover, we established ^{131}I-resistant DTC cells to explore the effect of circ_NEK6 on cell proliferation, apoptosis, migration, and invasion. Meanwhile, we also verified the mechanism by which circ_NEK6 regulated ^{131}I resistance in DTC via the miR-370-3p/MYH9 axis. Finally, we evaluated the role of circ_NEK6 in ^{131}I resistance *in vivo* using a tumor xenograft model and identified it as a novel target for the intervention and treatment of patients with DTC.

Materials and Methods

Clinical Samples

DTC tissue samples were obtained from 30 patients with the ^{131}I-resistant form and 30 patients with the ^{131}I-sensitive form at the Yunnan Cancer Hospital & The Third Affiliated Hospital of Kunming Medical University. The criteria for the ^{131}I-resistant group: (a) metastases that do not uptake iodine on whole-body imaging after the first ^{131}I treatment after successful nail clearance; (b) functional metastases that originally uptake iodine gradually lose iodine uptake after ^{131}I treatment; (c) partial metastases that uptake iodine and partial metastases that do not uptake iodine and can be revealed by other imaging examinations such as 18F-FDG PET/CT, CT or MRI; (d) iodine-intolerant metastases that maintain iodine uptake after multiple ^{131}I treatments but still progress within 1 year. The criteria for the ^{131}I-sensitive group: complete clearing of residual thyroid tissue after thyroid cancer surgery with ^{131}I treatment; complete clearing of metastatic lesions of thyroid cancer. Evidence and indications of successful ^{131}I treatment for DTC: (a) no radiological concentration in the thyroid bed on ^{131}I imaging; (b) no imaging evidence of tumor presence; (c) no serum Tg measured in the absence of TgAb interference is, in the case of thyroid hormone suppression therapy, and Tg < 1 μg/L in the case of TSH stimulation. The main baseline patient characteristics tabulated according to histological subtypes are provided in Additional file 1: Table S1. The tumor tissues samples were stored at -80°C until use. This study was authorized by Ethics Committee of The Yunnan Cancer Hospital & The Third Affiliated Hospital of Kunming Medical University. All participating patients provided written informed consent prior to enrollment in this study.

Cell Culture and Transfection

DTC cell lines (TPC-1, FTC-133, SW579, BCPAP, and K1), human thyroid follicular epithelial normal cell line Nthy-ori3-1, and HEK-293 T cell line were acquired from the BeNa Culture Collection (Beijing, China) and cultured in DMEM medium (Gibco) supplemented with 50 U/mL penicillin, 50 μg/mL streptomycin and 10% fetal bovine serum (Gibco) at 37°C in 5% CO_2. The circ_NEK6 shRNA (sh-NEK6), miR-370-3p mimic (miR-mimic), miR-370-3p inhibitor (mimic-NC), and MYH9 siRNA (si-MYH9) were purchased from GenePharma (Shanghai, China). The above vectors were incubated with Lipofectamine™ 3000 (Invitrogen, USA) according to the protocol.

[131]I-Resistant Cell Line Construction

To establish ^{131}I-resistant DTC cell lines (R-TPC-1 and R-BCPAP), both TPC-1 and BCPAP cells were incubated with an increasing dose of ^{131}I to acquire resistance according to the published article.[18] And the ^{131}I-resistant cell lines were treated with a median lethal dose of ^{131}I for 8 generations and the results showed in Figure S1.

Table 1. Name and Sequences of the Primers.

Name	Primer sequences
circ_NEK6	F: 5'-AAGAAGCAGAAGCGGCTCAT-3'
	R: 5'-ATGGATCCTCTCCGGTGACA-3'
miR-370-3p	F: 5'-ACACTCCAGCTGGGGCCTGCTGGG
	GTGGAACCT-3'
	R: 5'-CTCAACTGGTGTCGTGGA-3'
MYH9	F: 5'-AGAGCTCACGTGCCTCAACG-3'
	R: 5'-TGACCACACAGAACAGGCCTG-3'
U6	F: 5'-CTCGCTTCGGCAGCACA-3'
	R: 5'-AACGCTTCACGAATTTGCGT-3'
GAPDH	F: 5'-GGAAAGCTGTGGCGTGAT-3'
	R: 5'-AAGGTGGAAGAATGGGAGTT-3'

F: Forward primer; R: Reverse primer.

RNA Extraction and Quantitative Reverse Transcription-Polymerase Chain Reaction (qRT-PCR)

Total RNA was extracted from tissues or cells using TRIzol reagent (Invitrogen, USA), according to the manufacturer's protocol. RNA concentration was measured using a Nano-Drop2000c spectrophotometer (Thermo Fisher Scientific, USA). Reverse transcription was conducted to synthesize cDNA using a specific reverse transcription kit (TaKaRa, Japan). The internal control used for the detection of miR-370-3p was the expression of the small nuclear RNA, U6, while GAPDH was used as the internal control for detecting circ_NEK6 and MYH9 expressions. The relative expression levels were calculated using the $2^{-\Delta\Delta CT}$ methods. All primer sequences used are listed in Table 1.

3-(4, 5-Dimethyl-2-Thiazolyl)-2, 5-Diphenyl-2-H-Tetrazolium Bromide (MTT) Assay

Cell viability was measured using an MTT assay. Both R-TPC-1 and R-BCPAP cells (5×10^4 cells/well) were added into 96-well plates kept overnight, and incubated with different doses of ^{131}I for 24 h. Next, a medium containing 20 μL of MTT (5 mg/mL; Promega, USA) was added. Following incubation for 4 h, the medium was replaced with 200 μL of DMSO. The absorbance at 490 nm was detected using a microplate reader (Sunrise, TECAN, Inc., San Diego, CA, USA).

Flow Cytometry

Annexin V-FITC apoptosis kit (Solarbio, Beijing, China) was used to conduct the cell apoptosis assay through flow cytometry. Both R-TPC-1 and R-BCPAP cells (4×10^5 cells/well) were added into 12-well plates kept overnight, and treated with ^{131}I for 24 h. Then, the cells were collected using trypsin and were resuspended in the binding buffer. Next, the cells were dyed with 5 μL of Annexin V-FITC and propidium iodide (PI) for 10 min. Apoptotic cells were examined using a flow cytometer (Agilent, Hangzhou, China). The apoptotic rate is presented as the percentage of cells (Annexin V-FITC+ and PI-/+).

Transwell Assay

Transwell assay was conducted to examine the migratory and invasive abilities of both R-TPC-1 and R-BCPAP cells. For the Transwell assay with Matrigel, the 24-well Transwell plates (8-μm pore; Corning, USA) were coated with 25 mL of Matrigel (BD Biosciences, USA) and incubated for 1 h at 37°C before cell seeding. For both the Transwell assays with and without Matrigel, the transfected cells were trypsinized, then seeded into wells at a concentration of 10^5 cells per-well, and cultured in a medium with 2% fetal bovine serum. The bottom wells contained a normal growth medium with 10% fetal bovine serum. After 24 h, the migrated cells were fixed with 95% ethanol for 1 min and then air-dried. The cells were stained using crystal violet for 30 min, and cells in 3 random fields were counted under a microscope field (Olympus Corporation, Japan).

Western Blot Analysis

Total proteins were extracted from tissues or cells using RIPA lysis buffer (50 mM Tris-HCl pH 7.4, 150 mM NaCl, 1% NP40, 0.5% sodium deoxycholate, 0.1% sodium dodecyl sulfate; Beyotime, China) supplemented with a mixture of protease inhibitors at 4°C for 30 min. The protein concentration was measured through the Bradford protein assay (Bio-Rad, USA). Total protein was extracted through denaturation using 10% SDS-polyacrylamide gel electrophoresis. And then, the proteins were transferred onto the polyvinylidene fluoride membrane (Bio-Rad, Inc., USA). The membrane was blocked in 5% skimmed milk solution for 1 h at room temperature and incubated with the primary antibodies overnight at 4 °C, followed by further probed with the secondary antibody IgG-HRP (1:5000, Cell Signaling Technology, USA) for 1 h. Finally, the protein bands were visualized using an enhanced chemiluminescence system (Bio-Rad, USA). Protein levels were determined through normalization to GAPDH levels. The relative content of proteins in each group = gray value of target proteins/gray value of GAPDH. The primary antibodies for γ-H2AX (1:1000), MYH9 (1:1000), matrix metallopeptidase 2 (MMP-2; 1:1000), MMP-9 (1:1000), and GAPDH (1:1000) were all purchased from the Cell Signaling Technology (USA).

Dual-Luciferase Reporter Gene Assay

The wild-type sequence of circ_NEK6 or MYH9 3'UTR containing the binding sites for miR-370-3p were cloned into psiCHECK-2 (Promega, USA) to form the corresponding luciferase reporter vectors (wild type (WT)-circ_NEK6 and MYH9 3'UTR-WT). The mutant-types, MUT-circ_NEK6 and MYH9 3'UTR-MUT were obtained via mutating the seed sites. The constructed luciferase reporter vectors were co-transfected with a miR-370-3p mimic or miR-NC into HEK-293 T cells

to detect of luciferase activity using a dual-luciferase assay kit (Promega, USA).

Xenograft Model

A total of 30 BALB/c nude mice (female, 5-week-old) were obtained from Shanghai Kingbio Biosciences Inc. (Shanghai, China). The lentiviral vector carrying the short hairpin RNA for circ_NEK6 (sh-NEK6) or negative control (sh-NC) was synthesized via GenePharma (Shanghai, China). R-TPC-1 cells (1×10^7) stably transfected with sh-NEK6 or sh-NC were inoculated into flanks of the mice via subcutaneous injection. After 10 days, the mice were treated with ^{131}I at a dose of 2.0 mCi/100 g/d. Tumor volume was determined every 3 days and calculated as: Tumor volume (mm^3) = $1/2 \times$ length $\times$ width^2. Then, 27 days after injection, the mice were sacrificed via cervical dislocation. Tumor samples were weighed and harvested to examine the abundances of miR-370-3p, MYH9, MMP-2, and MMP-9.

Statistical Analysis

Each experiment was performed in triplicate. Numerical data are presented as the mean $\pm$ standard deviation. Pearson correlation analysis was conducted to detect the relevance between miR-370-3p and circ_NEK6 or MYH9. A paired or unpaired 2-tailed Student's t-test was used to compare differences between 2 groups of paired tissues or unpaired cells, respectively, while 1-way ANOVA followed by Tukey's post-hoc test was used to compare differences among multiple groups. Statistical analyses were conducted using SPSS 20.0 software (SPSS, Inc., USA), and a P-value of <0.05 was considered a statistically significant difference.

Results

circ_NEK6 Was Upregulated in ^{131}I-Resistant DTC Tissues and Cells

Several previous studies have demonstrated that the abnormal expression of circRNA was associated with radiotherapy tolerance of various malignant tumors.[19] circ_NEK6 expression was determined using qRT-PCR to explore its role in ^{131}I-resistant DTC. As shown in Figure 1A, circ_NEK6 expression was significantly higher in ^{131}I-resistant DTC tissues than ^{131}I-sensitive DTC tissues. In parallel, the expression of circ_NEK6 in DTC cell lines was higher than that of the human thyroid follicular epithelial normal cell line Nthy-ori3-1, and was exceptionally high in both TPC-1 and BCPAP cells (Figure 1B). Moreover, the expression of circ_NEK6 in ^{131}I-resistant DTC cells (R-TPC-1 and R-BCPAP) was higher than that of parental cells (TPC-1 and BCPAP; Figure 1C, 1D). These results indicated that circ_NEK6 upregulation might be associated with ^{131}I radioresistance in DTC.

Knockdown of circ_NEK6 Inhibited Cell Proliferation, Migration, Invasion, and Stimulated Cell Apoptosis in ^{131}I-Resistant DTC Cells

To explore the biological functions of circ_NEK6 in ^{131}I-resistant DTC cells, circ_NEK6 expression was knocked down via transfection of sh-circ_NEK6 (sh-NEK6) into both R-TPC-1 and R-BCPAP cells. The transfection efficacy was validated, as shown in Figure 2A. Moreover, knockdown of circ_NEK6 by enhancing the cytotoxicity of ^{131}I to both R-TPC-1 and R-BCPAP cells at the dose of 1.0 mCi/well and 0.5 mCi/well (Figure 2B), indicating that circ_NEK6 knockdown was declined both R-TPC-1 and R-BCPAP cells to ^{131}I resistance. Meanwhile, flow cytometry analysis results showed that knockdown of circ_NEK6 contributed to the sensitivity of both R-TPC-1 and R-BCPAP cells to ^{131}I by inducing cell apoptosis (Figure 2C-E). In addition, knockdown of circ_NEK6 significantly suppressed cell migration (Figure 2F, 2 H) and invasion (Figure 2G, 2I) in both R-TPC-1 and R-BCPAP cells under ^{131}I radiation. Furthermore, downregulation of circ_NEK6 significantly increased the protein level of the DNA damage marker, γ-H2AX, in both R-TPC-1 and R-BCPAP cells compared with that of the ^{131}I only treatment group (Figure 2 J, K). Overall, knockdown of circ_NEK6 promoted ^{131}I radiosensitivity of DTC cells by inhibiting cell proliferation, migration, invasion, and inducing cell apoptosis.

circ_NEK6 Negatively Regulated miR-370-3p Expression

The target gene of circ_NEK6 was predicted via StarBase V3.0 to explore the mechanism by which circ_NEK6 induces the development of ^{131}I-resistant DTC cells. The complementary sequence between circ_NEK6 and miR-370-3p is shown in Figure 3A. Moreover, qRT-PCR analysis results showed that the expression of miR-370-3p in ^{131}I-resistant DTC tissues was lower than in ^{131}I-sensitive DTC tissues (Figure 3B). Meanwhile, miR-370-3p expression was inversely associated with circ_NEK6 expression in ^{131}I-resistant DTC tissues (r = -0.5306, P = 0.0026; Figure 3C). Of note, we constructed WT-circ_NEK6 and MUT-circ_NEK6 to confirm the target correlation between circ_NEK6 and miR-370-3p. Upregulation of miR-370-3p markedly decreased the luciferase activity of WT-circ_NEK6, while this effect was abrogated in the MUT-circ_NEK6 group with mutated binding sites (Figure 3D). Furthermore, miR-370-3p expression was elevated via circ_NEK6 knockdown in both R-TPC-1 and R-BCPAP cells (Figure 3E). These findings indicated that circ_NEK6 could directly target and regulate miR-370-3p.

MYH9 Is a Target Gene of miR-370-3p

A bioinformatics database was used to predict the putative target gene of miR-370-3p, and MYH9 was identified (Figure 4A). Meanwhile, the mRNA level of MYH9 was found to be higher in ^{131}I-resistant DTC tissues than in ^{131}I-sensitive DTC tissues (Figure 4B). Interestingly, a negative correlation
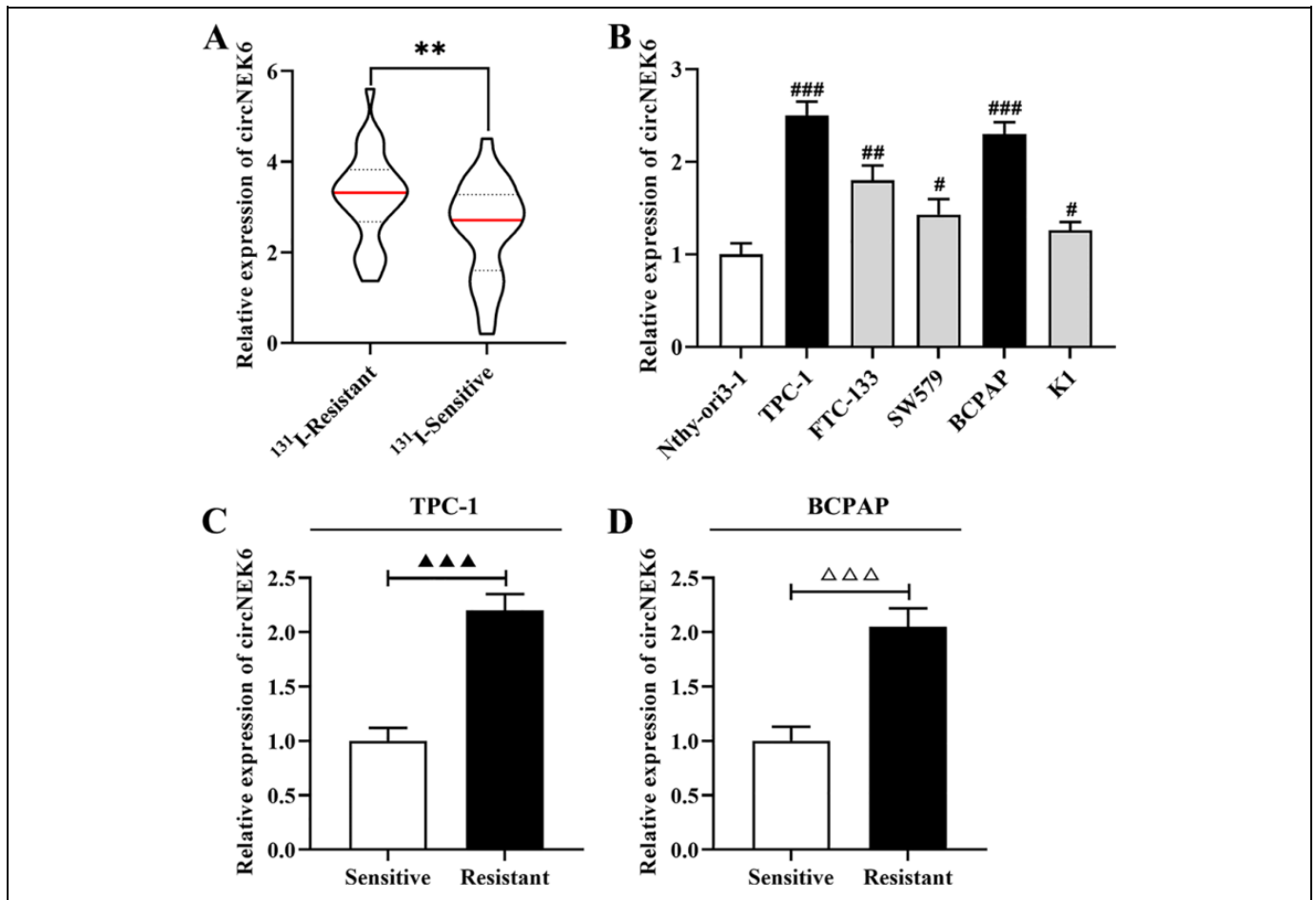
Figure 1. circ_NEK6 was upregulated in DTC tissues and cell lines. (A) The expression of circ_NEK6 in ^{131}I-resistant DTC tissues and ^{131}I-sensitive tissues was determined by qRT-PCR. (B) The expression of circ_NEK6 in the DTC cell lines and the human thyroid follicular epithelial normal cell line Nthy-ori3-1 was measured by qRT-PCR. qRT-PCR was used to detect the expression of circ_NEK6 in ^{131}I-resistant TPC-1 cells (C) and BCPAP cells (D) and their parent cells. **$P < 0.01$, compared with the ^{131}I-sensitive DTC tissues; [#]$P < 0.05$, [##]$P < 0.01$, [###]$P < 0.001$, compared with the Nthy-ori3-1 cells; [▲▲▲]$P < 0.001$, compared with the TPC-1 cells; [△△△]$P < 0.001$, compared with the BCPAP cells.

between miR-370-3p and MYH9 expression was determined using Pearson correlation analysis ($r = -0.4787$, $P = 0.0075$; Figure 4C). A luciferase reporter gene assay was conducted to verify MYH9 was a target of miR-370-3p. The results showed that overexpression of miR-370-3p suppressed the luciferase activity of the MYH9 WT construct, but not the mutated MYH9 construct, confirming that miR-370-3p targets MYH9 (Figure 4D). Furthermore, a significant reduction in MYH9 protein level expression was observed in both R-TPC-1 and R-BCPAP cells after transfection with the miR-370-3p mimic than in the miR-NC group (Figure 4E, 4F). These results indicated that MYH9 was a target gene of miR-370-3p.

Inhibition of circ_NEK6 Enhanced [131]I Radiosensitivity of DTC Cells by Upregulating the Inhibitory Effect of miR-370-3p on MYH9 Expression

To further probe the effect of circ_NEK6 knockdown on the malignant biological behavior of ^{131}I-resistant DTC cells via the regulation of the miR-370-3p/MYH9 axis. Western blot analysis was performed to detect the protein level of MYH9 in both R-TPC-1 and R-BCPAP cells when transfected with MYH9 siRNA (si-MYH9), si-MYH9+miR-370-3p inhibitor (miR-Inh), and miR-Inh+circ_NEK6 shRNA (sh-NEK6) before exposure to ^{131}I radiation. Following transfection with si-MYH9, the protein level of MYH9 decreased compared with the NC group (Figure 5A), while its expression increased after the simultaneous transfection of si-MYH9+miR-Inh or miR-Inh+sh-NEK6. Moreover, downregulation of MYH9 contributed to the sensitivity of both R-TPC-1 and R-BCPAP cells to ^{131}I by suppressing cell viability (Figure 5B) and inducing cell apoptosis (Figure 5C). However, knockdown of miR-370-3p significantly attenuated the silencing of circ_NEK6 or MYH9-mediated inhibition of ^{131}I resistance in both R-TPC-1 and R-BCPAP cells. Besides, miR-370-3p deficiency mitigated the knockdown of MYH9 or circ_NEK6-mediated suppression of migration (Figure 5D) and invasion (Figure 5E) in both R-TPC-1 and R-BCPAP cells. What's more, the knockdown of miR-370-3p attenuated the regulatory effect of silencing circ_NEK6 or MYH9 knockdown on the
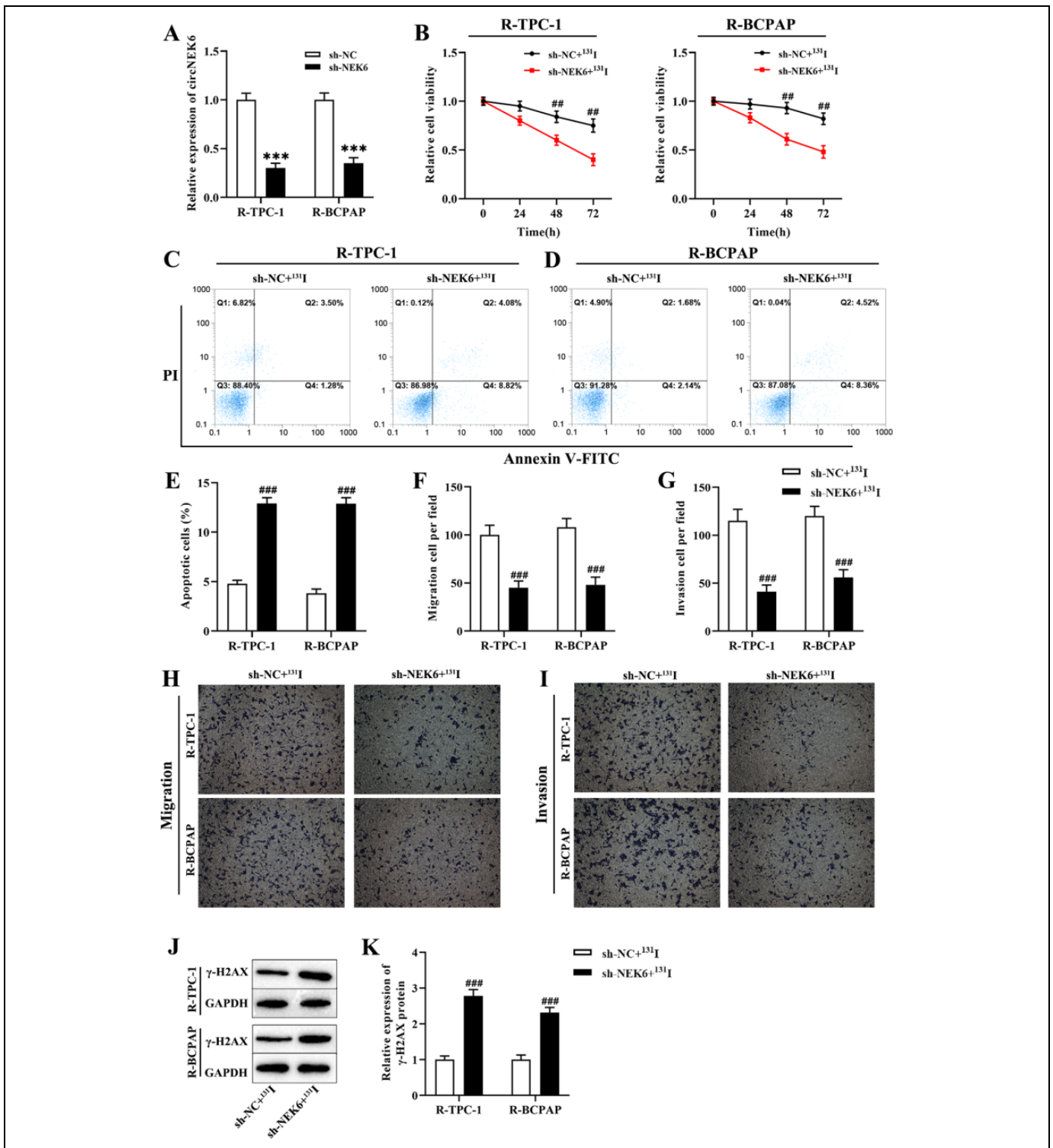
Figure 2. Knockdown of circ_NEK6 significantly inhibited cell proliferation, migration, and invasion, as well as promoted cell apoptosis and the expression of the γ-H2AX protein in both ^{131}I-resistant DTC cells. (A) qRT-PCR was employed to detect the expression of circ_NEK6 in both R-TPC-1 and R-BCPAP cells when transfected with circ_NEK6 shRNA (sh-NEK6) or sh-NC. Cell proliferation (B), cell apoptosis (C-E), migration (F and H), and invasion (G and I) were examined in both R-TPC-1 and R-BCPAP cells transfected with sh-NEK6 or sh-NC in the presence of 1 mCi/well and 0.5 mCi/well of ^{131}I treatment by MTT assay, flow cytometry, and Transwell assay, respectively. (J and K) Western blot was applied to detect the level of DNA damage marker γ-H2AX. ***$P < 0.001$, compared with the sh-NC group; $^{##}P < 0.01$, $^{###}P < 0.001$, compared with the sh-NC+^{131}I group.
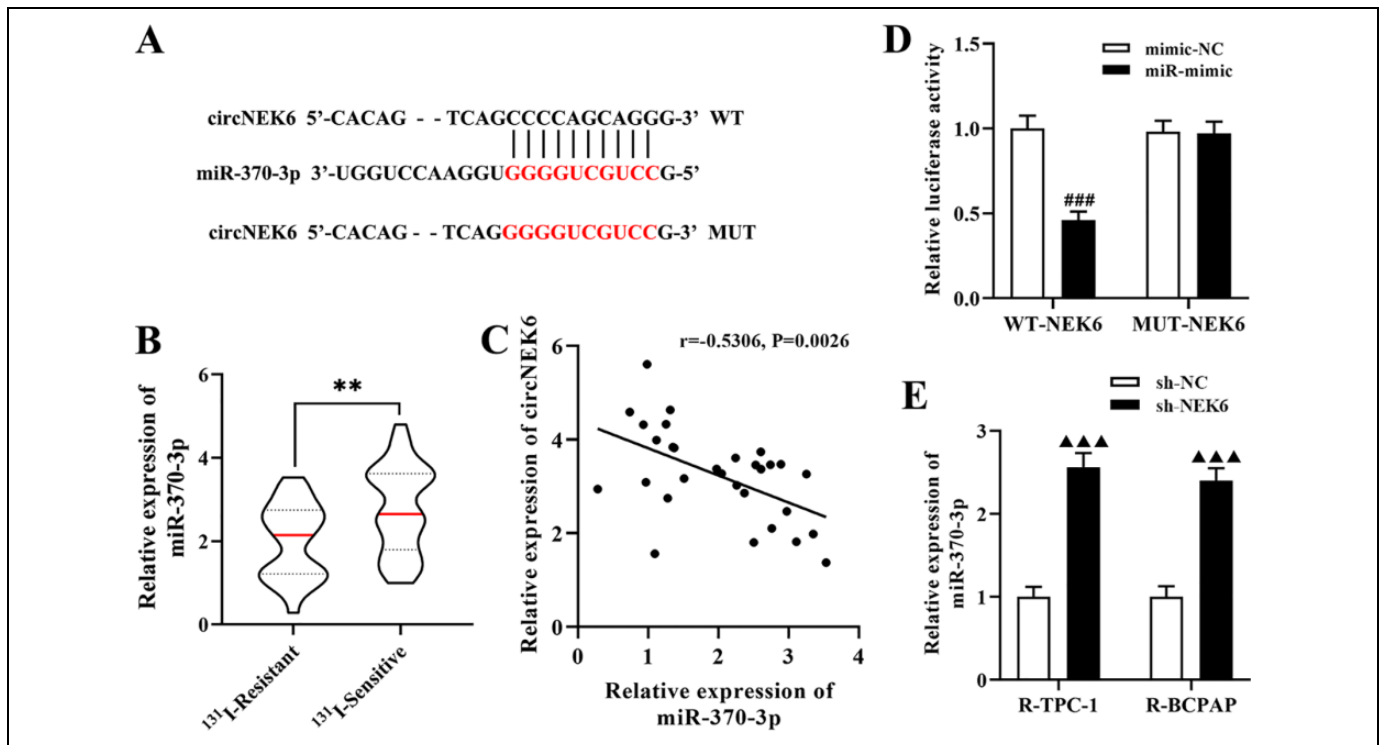
Figure 3. miR-370-3p was the target gene of circ_NEK6. (A) The target correlation between circ_NEK6 and miR-370-3p was explored via starBase. (B) qRT-PCR was used to the expression of miR-370-3p in ^{131}I-resistant DTC tissues and ^{131}I-sensitive tissues. (C) Pearson correlation analysis was conducted to detect the relevance between miR-370-3p and circ_NEK6. (D) Dual-luciferase reporter gene was employed to verify the association between circ_NEK6 and miR-370-3p. (E) miR-370-3p expression was detected in both R-TPC-1 and R-BCPAP cells transfected with sh-circ_NEK6 or sh-NC. **$P < 0.01$, compared with the ^{131}I-sensitive DTC tissues; ###$P < 0.001$, compared with the mimic-NC group; ▲▲▲$P < 0.001$, compared with the sh-NC group.

protein expression of the DNA damage marker, γ-H2AX (Figure 5F). These results suggested that circ_NEK6 inhibition enhanced the sensitivity of ^{131}I-resistant DTC cells to ^{131}I radiation by upregulating the inhibitory effect of miR-370-3p on the expression of MYH9.

Suppression of circ_NEK6 Promoted [131]I Radiosensitivity of DTC In Vivo

A tumor xenograft model was established by injecting nude mice with R-TPC-1 cells stably transfected with sh-NEK6, followed via ^{131}I treatment at a dose of 2.0 mCi/100 g/d to explore the effect of circ_NEK6 on ^{131}I resistance *in vivo*. As shown in Figure 6A-C, the sensitivity to ^{131}I of DTC xenograft tumor was enhanced by circ_NEK6 knockdown, as revealed by the aggravated reduction in tumor volume and weight. Moreover, tumor tissues were collected, and miR-370-3p expression and protein levels were detected. The qRT-PCR analysis showed that knockdown of circ_NEK6 significantly reduced miR-370-3p expression (Figure 6D), and MMP-2, MMP-9, and MYH9 protein levels (Figure 6E, 6F). In contrast, the protein level expression of γ-H2AX (Figure 6E, 6F) was markedly elevated in the sh-NEK6 group compared with the control group in the presence of [131]I. These results indicated that

circ_NEK6 inhibition decreased the ^{131}I resistance of DTC *in vivo*.

Discussion

Many clinical studies have confirmed that ^{131}I radiotherapy is an effective strategy for the treatment of patients with DTC.[20] However, the secondary radiation resistance of DTC cells to ^{131}I accelerates the proliferation and metastasis of tumor cells, resulting in ^{131}I implantation therapy, not delivering the expected therapeutic effect, or even resulting in failure. In the present study, our data showed that knockdown of circ_NEK6 reduced ^{131}I resistance of DTC *in vitro* and *in vivo*. Most importantly, suppression of circ_NEK6 inhibited the proliferation, migration, and invasion of ^{131}I-resistant DTC cells, and promoted cell apoptosis and increased the expression of the DNA damage marker, the γ-H2AX protein, via targeting upregulated the inhibitory effect of miR-370-3p on MYH9 expression.

Increasing evidence has demonstrated that circRNAs play pivotal roles in the development and progression of many tumors by regulating the malignant biological behavior of cancer cells.[21] Similarly, we published an article showing that circ_NEK6 overexpression contributed to cell proliferation and invasion, as well as decreased cell apoptosis in thyroid
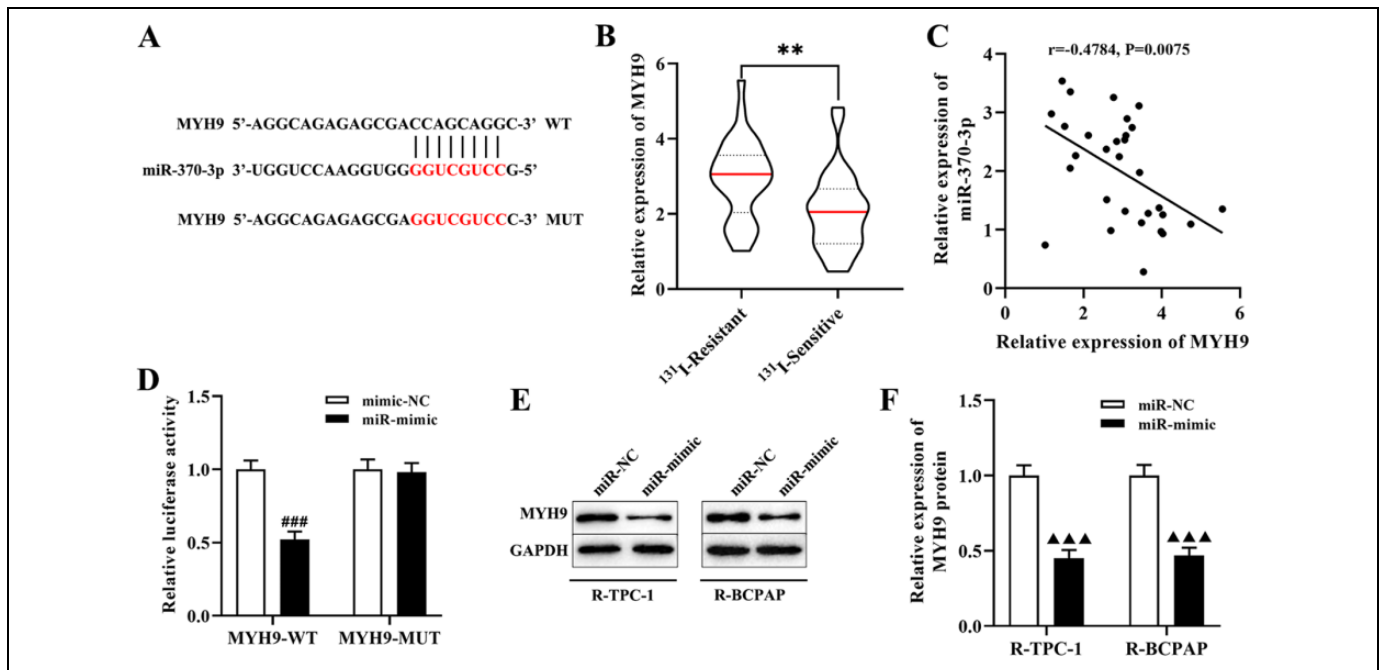
Figure 4. MYH9 was a target gene of miR-370-3p. (A) The target correlation between miR-370-3p and MYH9 was explored via starBase. (B) qRT-PCR was used to the mRNA expression of MYH9 in ^{131}I-resistant DTC tissues and ^{131}I-sensitive tissues. (C) Pearson correlation analysis was conducted to detect the relevance between miR-370-3p and MYH9. (D) miR-370-3p was predicted to bind to a sequence within the 3'-UTR of MYH9 mRNA. (E and F) Western blot was applied to examine the protein level of MYH9 in both R-TPC-1 and R-BCPAP cells transfected with miR-370-3p mimic (miR-mimic) or miR-NC. **$P < 0.01$, compared with the ^{131}I-sensitive DTC tissues; ###$P < 0.001$, compared with the mimic-NC group; ▲▲▲$P < 0.001$, compared with the miR-NC group.

cancer.[12] Previous studies found that abnormal circRNA is associated with the chemoresistance or radioresistance of malignant tumors, for example, Liu *et al* reported that circ_EIF6 knockdown significantly decreased the cisplatin-resistance of thyroid cancer cells by decreasing cell autophagy via sponging miR-144-3p.[22] Recent studies have found that circRNAs (including circ_CCDC66,[23] circ_000543,[24] and circ_001387[25]) are involved in cancer cell radiosensitization by inhibiting the malignant biological behavior of cancer cells. However, there is no direct evidence to support the association between circRNAs and the radioiodine resistance of DTC. In the present study, high circ_NEK6 expression was detected in ^{131}I-resistant DTC tissues and cell lines, implying that circ_NEK6 might be involved in the development of ^{131}I resistance in DTC. Of note, we found that the inhibitory effect of ^{131}I on resistant cell proliferation was enhanced when both ^{131}I-resistant DTC cells were transfected with circ_NEK6 shRNA. Moreover, tumor cell migration and invasion are 2 critical processes in resistant cells, contributing to radioresistance.[26] Similarly, our results showed that knockdown of circ_NEK6 distinctly decreased the migration and invasion abilities of ^{131}I-resistant DTC cells. What's more, DNA damage was an essential factor associated with radioresistance,[27] and our data showed that circ_NEK6 inhibition significantly enhanced the expression of the DNA damage marker, γ-H2AX. These results revealed that the knockdown of circ_NEK6 might be an effective treatment strategy for patients with ^{131}I-resistant DTC.

circRNAs have been confirmed to be associated with the tumorigenesis of cancer via targeting miRNAs and regulating mRNAs.[9] For instance, miR-370-3p is the target gene of circ_NEK6, which has been identified as a specific biomarker for diagnosing various cancers, including hepatocellular carcinoma,[28] bladder cancer,[29] colon adenocarcinoma.[30] Silencing of miR-370-3p significantly inhibited cancer cell proliferation, migration, and invasion, as well as induced cell apoptosis, for example, circAGFG1 accelerated cervical cancer progression by upregulating RAF1 via targeting miR-370-3p.[31] Wei *et al* found that circ_0020710 promoted tumor progression and immune evasion by regulating the miR-370-3p/CXCL12 axis in melanoma.[32] Moreover, miR-370-3p overexpression enhances the radiosensitivity of non-small cell lung cancer cells by suppressing proliferation and promoting cell apoptosis by targeting EGFR.[33] These results indicate that miR-370-3p may play an essential role in the radioiodine resistance of thyroid cancer by regulating cancer cell proliferation, apoptosis, and metastasis. Importantly, we demonstrated that miR-370-3p knockdown significantly alleviated the antiproliferation and anti-metastasis effect of circ_NEK6 or MYH9 on ^{131}I-resistant DTC cells.

Furthermore, MYH9, a target gene of miR-370-3p, acts as an oncogene in many solid cancers.[34] MYH9 inhibition significantly decreased the malignant phenotypes of cancer cells.[35] Additionally, MYH9 knockdown significantly attenuated cancer cell chemoresistance.[36] However, the effect of the
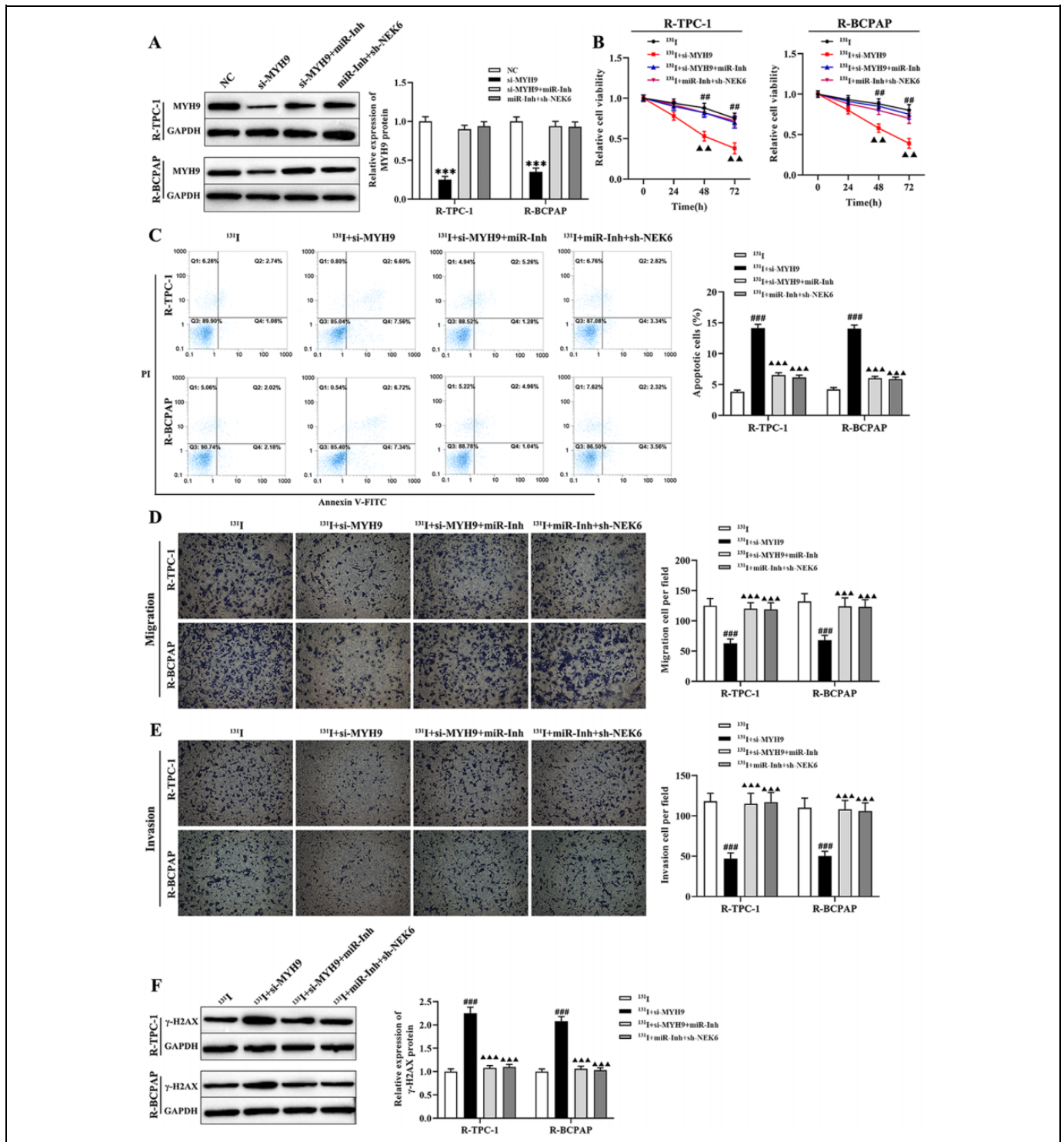
Figure 5. Knockdown of circ_NEK6 suppressed malignant phenotypes of ^{131}I-resistant DTC cells via the miR-370-3p/MYH9 axis. (A) Western blot was applied to examine the protein level of MYH9 in both R-TPC-1 and R-BCPAP cells transfected with MYH9 siRNA (si-MYH9), miR-370-3p inhibitor (miR-Inh), sh-NEK6. Cell proliferation (B), cell apoptosis (C), migration (D), and invasion (E) in both R-TPC-1 and R-BCPAP cells were examined by MTT assay, flow cytometry, and Transwell assay, respectively. (F) Western blot was applied to detect the level of γ-H2AX. ***$P < 0.001$, compared with the NC group; ##$P < 0.01$, ###$P < 0.001$, compared with the ^{131}I group; ▲▲$P < 0.01$, ▲▲▲$P < 0.001$, compared with the ^{131}I+si-MYH9 group.
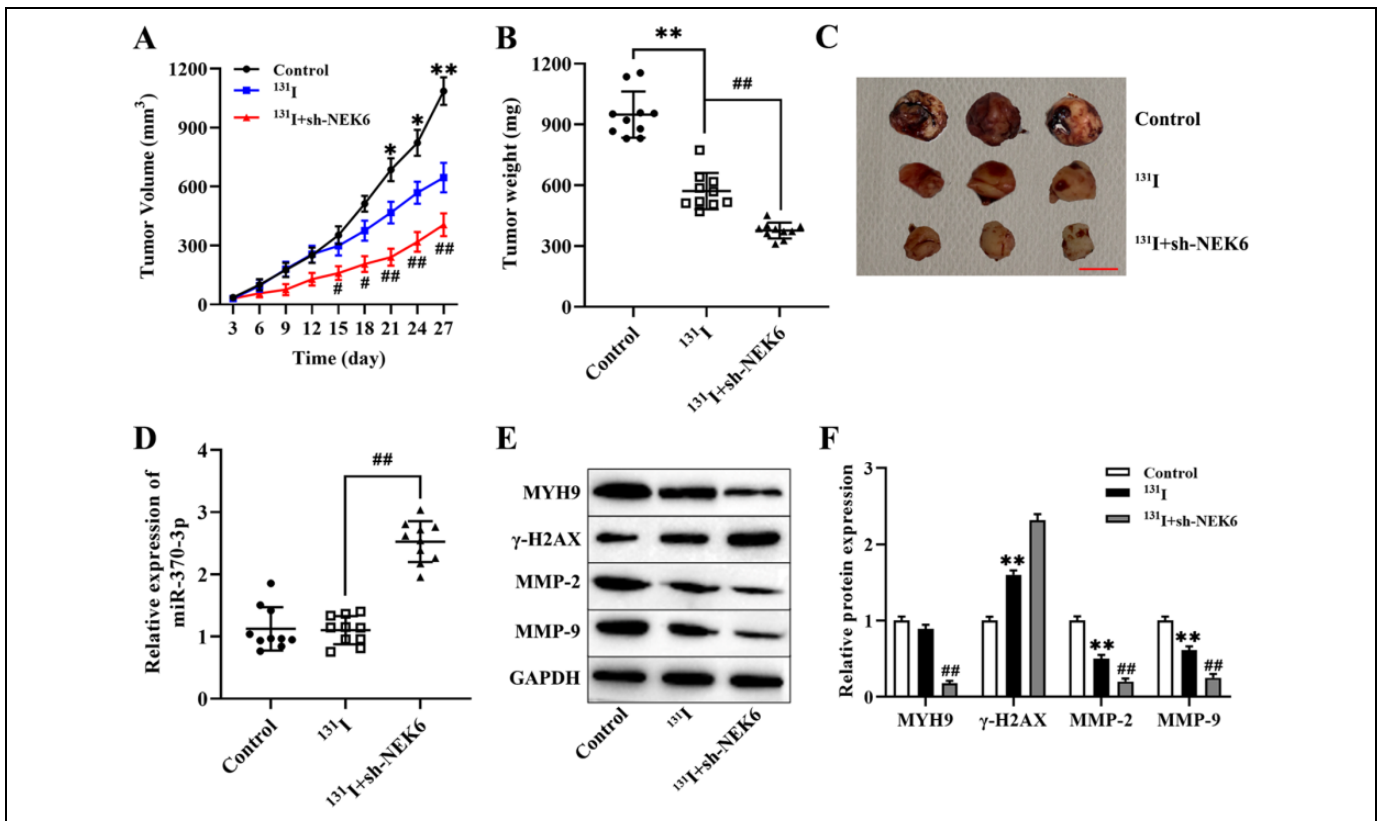
Figure 6. Knockdown of circ_NEK6 enhanced ^{131}I radiosensitivity of DTC *in vivo*. (A) Tumor volume was measured every 3 days from ^{131}I treatment on the 10th day (n = 10 mice/group). (B) The subcutaneous tumor quality was measured after the mice were killed in each group. (C) Representative image of tumors of mice in each group, Scale bar = 1.0 cm. (D) qRT-PCR was used to detect the expression of miR-370-3p in tumor tissues. (E and F) Western blot was applied to examine the protein levels of MYH9, γ-H2AX, MMP-2, and MMP-9 in tumor tissues derived from a different group. *$P < 0.05$, **$P < 0.01$, compared with the control group; #$P < 0.05$, ##$P < 0.01$, compared with the ^{131}I group.

miR-370-3p/MYH9 axis on ^{131}I resistance is not yet fully elucidated. In this study, our data showed that knockdown of MYH9 could inhibit the proliferation, migration, and invasion of ^{131}I-resistant DTC cells, and also facilitated cell apoptosis. Collectively, these results indicated that the circ_NEK6/miR-370-3p/MYH9 axis might be an effective therapeutic agent for ^{131}I-resistant DTC patients.

However, there are some deficiencies in this article. Firstly, in the mechanism research, other downstream targets of circ_NEK6 need to be further screened and verified, which will further clarify the downstream mechanism of circ_NEK6; Secondly, to explore the value of circ_NEK6 as a prognostic marker, more patients, together with corresponding follow-up information, should be included to analyze the overall survival time and relapse-free survival time. In addition, due to the limitation of sample size, it is necessary to carry out further research in a larger research queue. Importantly, the results of this study demonstrate that circ_NEK6 is upregulated in ^{131}I-resistant DTC tissues and cell lines. Moreover, circ_NEK6 suppression inhibited the proliferation, invasion, and migration abilities of ^{131}I-resistant DTC cells *in vitro* and *in vivo*, potentially by downregulating MYH9 via targeting miR-370-3p. Therefore, this study may provide novel insights into

radioiodine resistance and has identified a potential novel target that can be used to improve radioiodine-therapy of DTC.

Authors' Note

Zhiyong Deng and Jiaping Wang designed the experiments. Fukun Chen, Zhiping Feng, Chao Liu, and Juan Lv performed experiments. Fukun Chen, Shuting Yin, Yuanjiao Chen, and Ruoxia Shen analyzed data. Fukun Chen and Shuting Yin drafted the manuscript. Zhiyong Deng and Jiaping Wang revised manuscript. All authors read and approved the final manuscript. The analyzed data sets generated during the study are available from the corresponding author on reasonable request. Our study was approved by the Ethics Committee of The Yunnan Cancer Hospital & The Third Affiliated Hospital of Kunming Medical University (approval no. KY201848). All patients provided written informed consent prior to enrollment in the study. Fukun Chen and Shuting Yin contributed equally to this work.

Declaration of Conflicting Interests

Funding

ORCID iD

Zhiyong Deng ⓘ https://orcid.org/0000-0002-4933-9772

Supplemental Material

Supplemental material for this article is available online.

References

1. Burton BN, Okwuegbuna O, Jafari A, et al. Association of pre-operative anemia with 30-day morbidity and mortality among patients with thyroid cancer who undergo thyroidectomy. *JAMA Otolaryngol Head Neck Surg*. 2019;145(2):124-131.

2. Carling T, Udelsman R. Thyroid cancer. *Annu Rev Med*. 2014;65: 125-137.

3. Berdelou A, Lamartina L, Klain M, et al. Treatment of refractory thyroid cancer. *Endocr Relat Cancer*. 2018;25(4): R209-r223.

4. Yang X, Liang J, Li TJ, et al. Postoperative stimulated thyroglobulin level and recurrence risk stratification in differentiated thyroid cancer. *Chin Med J (Engl)*. 2015;128(8): 1058-1064.

5. Luo X, Wu A. Analysis of risk factors for postoperative recurrence of thyroid cancer. *J buon*. 2019;24(2):813-818.

6. Jerkovich F, García Falcone MG, Pitoia F. The experience of an endocrinology division on the use of tyrosine multikinase inhibitor therapy in patients with radioiodine-resistant differentiated thyroid cancer. *Endocrine*. 2019;64(3):632-638.

7. Capdevila J, Galofré JC, Grande E, et al. Consensus on the management of advanced radioactive iodine-refractory differentiated thyroid cancer on behalf of the Spanish Society of Endocrinology Thyroid Cancer Working Group (GTSEEN) and Spanish Rare Cancer Working Group (GETHI). *Clin Transl Oncol*. 2017; 19(3):279-287.

8. Kristensen LS, Hansen TB, Venø MT, Kjems J. Circular RNAs in cancer: opportunities and challenges in the field. *Oncogene*. 2018; 37(5):555-565.

9. Verduci L, Strano S, Yarden Y, Blandino G. The circRNA-microRNA code: emerging implications for cancer diagnosis and treatment. *Mol Oncol*. 2019;13(4):669-680.

10. Yang C, Wei Y, Yu L, Xiao Y. Identification of altered circular RNA expression in serum exosomes from patients with papillary thyroid carcinoma by high-throughput sequencing. *Med Sci Monit*. 2019;25:2785-2791.

11. Peng N, Shi L, Zhang Q, et al. Microarray profiling of circular RNAs in human papillary thyroid carcinoma. *PLoS One*. 2017; 12(3):e0170287.

12. Chen F, Feng Z, Zhu J, et al. Emerging roles of circRNA_NEK6 targeting miR-370-3p in the proliferation and invasion of thyroid cancer via Wnt signaling pathway. *Cancer Biol Ther*. 2018; 19(12):1139-1152.

13. Didiano D, Hobert O. Molecular architecture of a miRNA-regulated 3' UTR. *Rna*. 2008;14(7):1297-1317.

14. Barbato S, Solaini G, Fabbri M. MicroRNAs in oncogenesis and tumor suppression. *Int Rev Cell Mol Biol*. 2017;333:229-268.

15. Shen X, Zuo X, Zhang W, et al. MiR-370 promotes apoptosis in colon cancer by directly targeting MDM4. *Oncol Lett*. 2018; 15(2):1673-1679.

16. Wang Y, Ma DL, Yu CH, et al. MicroRNA-370 suppresses SOX12 transcription and acts as a tumor suppressor in bladder cancer. *Eur Rev Med Pharmacol Sci*. 2020;24(5):2303-2312.

17. Liu L, Yi J, Deng X, et al. MYH9 overexpression correlates with clinicopathological parameters and poor prognosis of epithelial ovarian cancer. *Oncol Lett*. 2019;18(2):1049-1056.

18. Liu C, Feng Z, Chen T, et al. Downregulation of NEAT1 reverses the radioactive iodine resistance of papillary thyroid carcinoma cell via miR-101-3p/FN1/PI3K-AKT signaling pathway. *Cell Cycle*. 2019;18(2):167-203.

19. Cui C, Yang J, Li X, et al. Functions and mechanisms of circular RNAs in cancer radiotherapy and chemotherapy resistance. *Mol Cancer*. 2020;19(1):58.

20. Ciarallo A, Rivera J. Radioactive iodine therapy in differentiated thyroid cancer: 2020 update. *AJR Am J Roentgenol*. 2020; 215(2)285-291.

21. Patop IL, Kadener S. circRNAs in cancer. *Curr Opin Genet Dev*. 2018;48:121-127.

22. Liu F, Zhang J, Qin L, et al. Circular RNA EIF6 (Hsa_circ_0060060) sponges miR-144-3p to promote the cisplatin-resistance of human thyroid carcinoma cells by autophagy regulation. *Aging (Albany NY)*. 2018;10(12):3806-3820.

23. Wang L, Peng X, Lu X, et al. Inhibition of hsa_circ_0001313 (circCCDC66) induction enhances the radio-sensitivity of colon cancer cells via tumor suppressor miR-338-3p: effects of cicr_0001313 on colon cancer radio-sensitivity. *Pathol Res Pract*. 2019;215(4):689-696.

24. Chen L, Zhou H, Guan Z. CircRNA_000543 knockdown sensitizes nasopharyngeal carcinoma to irradiation by targeting miR-9/platelet-derived growth factor receptor B axis. *Biochem Biophys Res Commun*. 2019;512(4):786-792.

25. Shuai M, Huang L. High expression of hsa_circRNA_001387 in nasopharyngeal carcinoma and the effect on efficacy of radiotherapy. *Onco Targets Ther*. 2020;13:3965-3973.

26. Li YH, Xu CL, He CJ, et al. circMTDH.4/miR-630/AEG-1 axis participates in the regulation of proliferation, migration, invasion, chemoresistance, and radioresistance of NSCLC. *Mol Carcinog*. 2020;59(2):141-153.

27. Qiu GH. Protection of the genome and central protein-coding sequences by non-coding DNA against DNA damage from radiation. *Mutat Res Rev Mutat Res*. 2015;764:108-117.

28. Yu Y, Xu P, Cui G, et al. UBQLN4 promotes progression of HCC via activating wnt-β-catenin pathway and is regulated by miR-370. *Cancer Cell Int*. 2020;20:3.

29. Huang X, Zhu H, Gao Z, et al. Wnt7a activates canonical Wnt signaling, promotes bladder cancer cell invasion, and is suppressed by miR-370-3p. *J Biol Chem*. 2018;293(18):6693-6706.

30. Wei Y, Shao J, Wang Y, et al. Hsa-miR-370 inhibited P-selectin-induced cell adhesion in human colon adenocarcinoma cells. *Mol Cell Biochem*. 2019;450(1-2):159-166.

31. Wu F, Zhou J. CircAGFG1 promotes cervical cancer progression via miR-370-3p/RAF1 signaling. *BMC Cancer*. 2019;19(1):1067.

32. Wei CY, Zhu MX, Lu NH, et al. Circular RNA circ_0020710 drives tumor progression and immune evasion by regulating the miR-370-3p/CXCL12 axis in melanoma. *Mol Cancer*. 2020; 19(1):84.

33. Liu AM, Zhu Y, Huang ZW, et al. Long noncoding RNA FAM201A involves in radioresistance of non-small-cell lung cancer by enhancing EGFR expression via miR-370. *Eur Rev Med Pharmacol Sci*. 2019;23(13):5802-5814.

34. Lin X, Yu GF, Zuo S, et al. Low MYH9 expression predicts a good prognosis for hepatocellular carcinoma. *Int J Clin Exp Pathol*. 2018;11(5):2784-2791.

35. Wang B, Qi X, Liu J, et al. MYH9 promotes growth and metastasis via activation of MAPK/AKT signaling in colorectal cancer. *J Cancer*. 2019;10(4):874-884.

36. Paciullo F, Bury L, Gresele P. Eltrombopag to allow chemotherapy in a patient with MYH9-related inherited thrombocytopenia and pancreatic cancer. *Int J Hematol*. 2020;112(5): 725-727.